Materials Science-Poland, 38(1), 2020, pp. 143-150
http://www.materialsscience.pwr.wroc.pl/
DOI: 10.2478/msp-2019-0091

Synthesis of PMMA-$HoVO_4$ nanocomposites by emulsifier-free emulsion polymerization: radical effects

B. Bulbul, E.Y. Pekcaliskan[1], S. Beyaz*

[1]Department of Chemistry, Faculty of Science&Literature, Balıkesir University, Balıkesir, Turkey

Poly(methyl methacrylate)-holmium orthovanadate (PMMA-$HoVO_4$) nanocomposites were synthesized using emulsifier-free emulsion polymerization system in two ways. In the first one, the $HoVO_4$ nanoparticle dispersion was added to the emulsion system before or after polymerization start (*in situ* polymerization). In the other one, nanoparticle dispersion and polymeric latex were mixed together at room temperature (blending). Crystalline $HoVO_4$ nanoparticles (about 60 nm) were synthesized by co-precipitation method. Three different composite latexes were synthesized by varying the potassium persulfate concentration and the time of $HoVO_4$ nanoparticles addition. According to the dynamic light scattering analysis, the size of the polymer beads in the latexes is between 244.8 nm and 502.5 nm and the PDI values are in the range of 0.005 to 0.206. Infrared spectral analysis showed that $HoVO_4$ caused some changes in the structure of the polymer. Luminescence measurements attempted to determine optical properties of the nanocomposites. The results have shown that $HoVO_4$ nanoparticles do not protect their structure due to the reaction with persulfate radicals but that they enter the polymer beads and change the luminescence properties of the polymer forming a new material with different properties.

Keywords: *PMMA; nanocomposite; holmium orthovanadate; emulsion polymerization*

1. Introduction

The development of polymer-based composites that display various optical functionalities, such as high/low refractive index, tunable absorption/emission characteristics, is of great interest due to potential optoelectronic applications [1, 2]. While the polymeric component provides processability, flexibility and transparency, inorganic particles contribute to the desired optical properties. Due to its optical clarity and known chemical and physical properties, poly(methyl methacrylate) (PMMA, Plexiglas) is a perfect host for functional particles. Various types of metal oxide fillers, such as TiO_2 [3], Nb_2O_5 [4] and lanthanide-doped inorganic nanoparticles such as YVO_4 [5], CeF_3 [6], $NaYF_4$ [7], Y_2O_3 [8] have been incorporated into PMMA to modify the optical properties of these polymers. There are many reports describing the preparation of polymer latex composites [9–11]. A suitable method for the preparation of such nanocomposites is in situ polymerization of particle dispersions. For this route, a stable dispersion of inorganic particles is necessary in the polymerization medium. Particle aggregation or growth can cause loss of transparency in the resulting polymers due to scattering of light. But there are few examples of nanoparticle incorporation into uniform polymer microparticles.

Holmium orthovanadate ($HoVO_4$) is known for its strong magnetic and luminescence properties [12]. Due to short ion relaxation time, holmium is commonly used in electrical, electronic and data transfer systems, but laser applications are also noteworthy due to the fact that they have spectrum bands in the visible and near infrared regions [13, 14]. We have not found any study on the use of $HoVO_4$ nanoparticles as a filler in PMMA nanocomposites. In our investigations, it was determined that the $HoVO_4$ nanoparticles were highly stable in water. Thus, without agglomeration, their aqueous dispersions can be added to the emulsifier-free emulsion polymerization system of methyl methacrylate in order to form ideal PMMA nanocomposites.

---

*E-mail: sedacan@balikesir.edu.tr

In this study, PMMA-$HoVO_4$ nanocomposites were prepared by emulsifier-free emulsion polymerization of methyl methacrylate in the presence of $HoVO_4$ nanoparticles. For comparison, pure PMMA latex was also synthesized. In addition, a blending method was employed to better understanding radical effects. The properties of the latexes were discussed by the analysis of results of dynamic light scattering, electron microscopy, infrared spectroscopy and photoluminescence spectroscopy.

2. Experimental

2.1. Materials

Holmium nitrate ($Ho(NO_3)_3{\cdot}5H_2O$), sodium hydroxide (NaOH) and amonium metavanadate (NH_4VO_3) were purchased from Merck Company and used as received without further purification. Methyl methacrylate (MMA) was also purchased from Merck It was freed from phenolic inhibitors by shaking with 5 % (w/v) aqueous NaOH, washing with water, and drying over Na_2SO_4. The initiator, potassium persulfate (KPS), was a product of Fluka, Germany.

2.2. Preparation of holmium orthovanadate nanoparticles and aqueous dispersion

$HoVO_4$ nanoparticles were synthesized by a coprecipitation method from solution [12]. 0.480 g NaOH and 0.468 g NH_4VO_3 were added to 20 mL of water to form Na_3VO_4 aqueous solution (A). The lanthanide solution (B) was also prepared in 20 mL water using 1.764 g of holmium nitrate. Solution B was added to the solution A in the reaction vessel. The reaction was allowed to continue for 30 min under a stirring rate of 2000 rpm. Finally, the precipitate was formed at room temperature. It was washed with ethanol 3 times and deionized water, one time using a centrifuge for 5 min at 5000 rpm. 500 mL of deionized water was added to the separated sediment to prepare a stable aqueous dispersion (Fig. 1). The pH of the final solution was measured as 9.68. The prepared dispersion was stable for weeks. The solids content in the prepared $HoVO_4$ aqueous dispersion was gravimetrically determined and found to be 1.75×10^{-3} g/mL.

2.3. Synthesis of poly(methyl methacrylate)-$HoVO_4$ nanocomposites

Polymerization was carried out at 70 °C in a 500 mL round-bottom three-neck glass flask equipped with a nitrogen inlet, thermometer (±0.1 °C), and condenser. The reactor was immersed in a thermostated water bath to maintain a constant temperature. First, 450 mL of water and 9.4 g of MMA were charged into the reactor and stirred under nitrogen atmosphere for about 60 min to remove oxygen from the reaction system. Temperature equilibrium was attained and the aqueous phase was saturated with monomer. The defined amount of KPS dissolved in 40 mL water, was added into the reactor. The polymerization was performed at 300 rpm (magnetic stirrer) for about 90 min. 140 mL of $HoVO_4$ aqueous dispersion was added into the polymerization system before/after the polymerization started. The total reaction volume was kept constant at 490 mL. Polymerization recipes were summarized in Table 1.

After the polymerization started, 10 mL of the latex was removed from the reactor at specific time intervals. It was poured into glass vial containing 1% hydroquinone as an inhibitor. The final product was dried in an oven at 70 °C. The monomer conversion (X %) was calculated by equation 1:

$$X\% = \frac{m_L - m_N \cdot W_H}{m_N \cdot W_s - m_N \cdot W_H} \qquad (1)$$

where m_L is the weight of latex solution taken from reactor; m_N, the weight of dry polymer; W_H and W_S, the weight fractions of holmium orthovanadate and solid initially in the reaction mixture, respectively.

Blending method 5 mL of pure PMMA latex and 5 mL of $HoVO_4$ dispersion were mixed together at 500 rpm for 15 min.

2.4. Characterization

The crystalline structure of $HoVO_4$ nanoparticles was investigated with Rigaku Rint 2200 XRD Analyzer with CuKα radiation (1.54059 Å)

Table 1. Experimental polymerization recipes and sample labels.

Sample	Water [mL]	KPS [g]	Adding way of HoVO$_4$ aqueous dispersion
PMMA	450	0.257	Not added
P1	310	0.257	Before polymerization started
P2	310	0.514	Before polymerization started
P3	310	0.257	Dropped at 2 – 3 min of polymerization

at 30 mA and 40 kV. FT-IR spectra were recorded using PerkinElmer 65 model FT-IR spectrometer in the range of 4000 cm^{-1} to 600 cm^{-1}. Transmission electron microscopy investigations were performed on JEOL-2100 HRTEM operating at 200 kV (LaB$_6$ filament). Images were taken by Gatan Model 794 Slow Scan CCD Camera and also by Gatan Model 833 Orius SC200D CCD Camera. Copper TEM grids (Electron Microscopy Sciences, CF200-Cu, 200 mesh) coated with carbon film were used. The surface charges and hydrodynamic radius of the particles were measured using Zetasizer NanoZS (Malvern Instruments). Before measurement, the particles were diluted about 100 times with deionized water; thereafter, the samples were introduced into a thermostated scattering cell at 25 °C. SEM images were taken by JEOL SEM-7100-EDX operating at 20 kV. Luminescence measurements were carried out at the room temperature and excitation densities between 0.01 W/cm^2 and 1.04 W/cm^2 by using Teledyne Tekmar US12201001Atomx.

3. Results and discussion

Fig. 1 shows that colors of the prepared HoVO$_4$ nanopowders and nanodispersions change upon exposure to different wavelength of light (fluorescent, daylight, UV) which indicates photochromism. Thus, it can be said that HoVO$_4$ nanoparticles is a photochromic material like BiVO$_4$ [15]. The HoVO$_4$ nanoparticles, stimulated by fluorescent light, 450 nm, radiated at 650 nm due to $^5F_5 \rightarrow {}^5I_8$ transition, while the ones, excited by fluorescent light, 365 nm, radiated at 550 nm due to $^5S_2 \rightarrow {}^5I_8$ transition [13].

Fig. 1. HoVO$_4$ nanopowders and nanodispersions under fluorescent light 450 nm (1), fluorescent light 365 nm (2), daylight (3), and UV radiation (4).

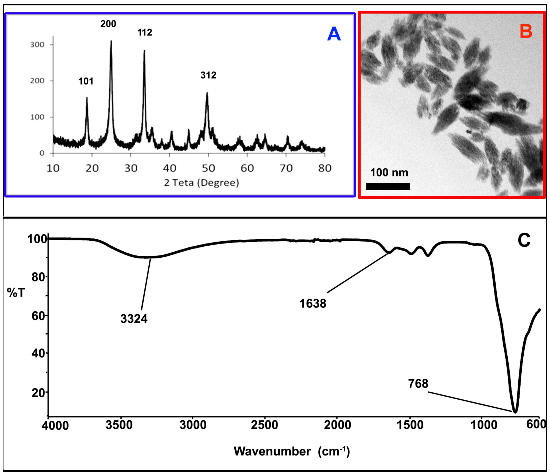

Fig. 2. (A) XRD pattern, (B) HRTEM image and (C) FT-IR spectrum of HoVO$_4$ nanoparticles.

XRD pattern of the as-prepared nanoparticles (Fig. 2A) can be indexed to tetragonal phase of zircon type orthovanadate with cell parameters HoVO$_4$: a = b = 7.122 Å, c = 6.289 Å, which is in good agreement with the literature value (JCPDS

Card No.: 82-1973) [16]. No other impurities were detected in the synthesized product and it was found to be of very good crystallinity. In Fig. 2B, typical high resolution TEM images (HRTEM) display spindle-like particles which have a length of about 60 nm and a width of about 30 nm. FT-IR was performed on the as-prepared $HoVO_4$ nanoparticles and illustrated in Fig. 2C. The sample contains a strong absorption band at 768 cm^{-1} that can be attributed to the adsorption of V–O (from the VO_4^{3-} group) [17]. The absorption bands located at 3324 cm^{-1} and 1638 cm^{-1} can be ascribed to O–H stretching and bending vibration of water [18].

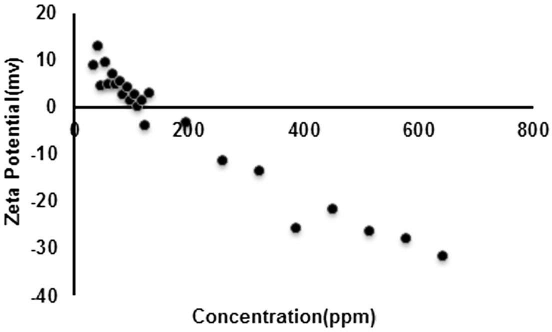

Fig. 3. Zeta potential values of $HoVO_4$ nanoparticles vs. their concentration in water.

A homogenous distribution of nanoparticles in a polymerization medium is an important criterion for the synthesis of an ideal nanocomposite. Therefore, it is necessary to determine the surface charge of $HoVO_4$ nanoparticles in water and the concentration at which they remain stable. As seen from Fig. 3, the surface charge of the nanoparticles in the concentration range of 400 ppm to 600 ppm is around –30 mV, which is sufficient for stability. Thus, the polymerization medium was adjusted to have a $HoVO_4$ concentration of 500 ppm in water.

PMMA-$HoVO_4$ nanocomposites obtained by adding $HoVO_4$ dispersions by different ways are shown in Table 1. A polymerization without any nanoparticle was also carried out for comparison.

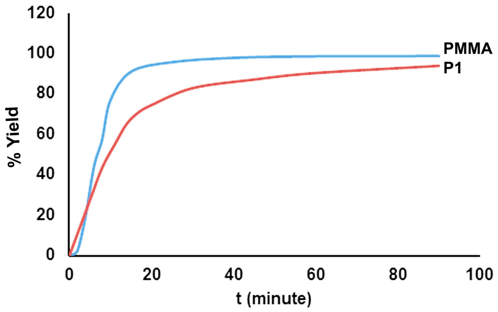

Fig. 4. Polymerization kinetics of pure PMMA and PMMA containing $HoVO_4$ nanoparticles.

3.1. Effect of $HoVO_4$ nanoparticles on the kinetics of PMMA polymerization

Using the % yield values of PMMA and P1 samples, the time dependent kinetic curves of the polymerization were given in Fig. 4. The conversion of pure PMMA reached 90 % in 15 min. At the end of 90 min, it was almost 99 %. It was observed that the addition of the $HoVO_4$ nanoparticles to the polymerization solution resulted in slowing down the polymerization and reduction of the conversion rate at the end of 90 min. This may be because the nanoparticles change their initiator activity negatively. It is known that vanadium ions react with persulfate and are used in the activation of persulfate [19, 20]:

$$V^{+5} + S_2O_8^{2-} \rightarrow V^{+4} + S_2O_8^{-} \qquad (2)$$

Excessive radical production leads to an increase in radical termination and salt amount. Another effect that may cause polymerization to slow down is also the salt effect [21].

3.2. Morphologies of PMMA-$HoVO_4$ latexes

In the synthesis of PMMA-$HoVO_4$ nanocomposites, the nanoparticles were added into polymerization using different ways: before/after polymerization started. In addition, composite latex synthesis was performed by increasing the amount of initiator in order to observe the radical effects better. The bead size and surface charges of synthesized latex composites and pure PMMA latex were measured by Zetasizer NanoZS and summarized in Table 2. According to the obtained results, the latex size of the P1 is bigger than that of the pure PMMA latex. This can be also explained by the reduction of radicals which leads to decrease in the surface charge of the particles [22]. Another reason may be a decrease in the monomer solubility due to HoVO$_4$ nanoparticles [23]. The surface charge of the P2 latex synthesized using higher initiator amount is higher than those of PMMA and P1 latex and the particle size is larger due to the salt effect [21]. To minimize the effect of vanadium-persulfate interaction, the persulfate initiator was first added to the polymerization system, then the HoVO$_4$ dispersion was rapidly introduced from the burette and P3 composite latex was obtained. The latex size of P3 was found smaller than the size of P1 and PMMA latex since the nanoparticles behaved like a nucleus and caused the increasing of particles number [24]. However, the PDI value of P3 latex was higher than of the other samples. It can be said that the nanoparticles, which were added later, disrupted the equilibrium and uniformity in the system.

Table 2. Z-average hydrodynamic radius and surface charge of the latex composites.

Sample	D_L [nm]	PDI	Zeta [mV]
PMMA	262.4	0.005	–42.5
P1	401.5	0.032	–36.8
P2	502.5	0.055	–48.8
P3	244.8	0.106	–37.5

High resolution TEM analysis was performed to better examine the morphologies of the synthesized composite latexes. The PMMA was melting during the analysis due to electrons with high energy as seen in Fig. 5. Therefore, it may be difficult to comment on the composite structure. However, there is an interesting result from the TEM analysis: the shape of the nanoparticles inside the composite has turned to the sphere and its dimensions have reduced to around 20 nm to 30 nm. This result demonstrates that HoVO$_4$ nanoparticles react clearly with the species in the medium during polymerization.

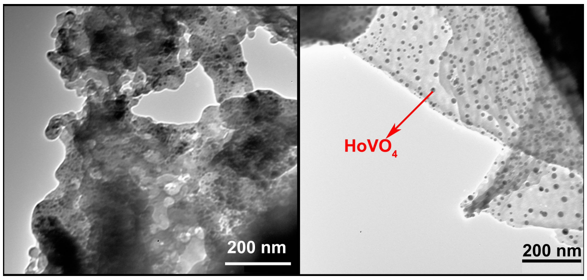

Fig. 5. HRTEM images of P1 composite latex.

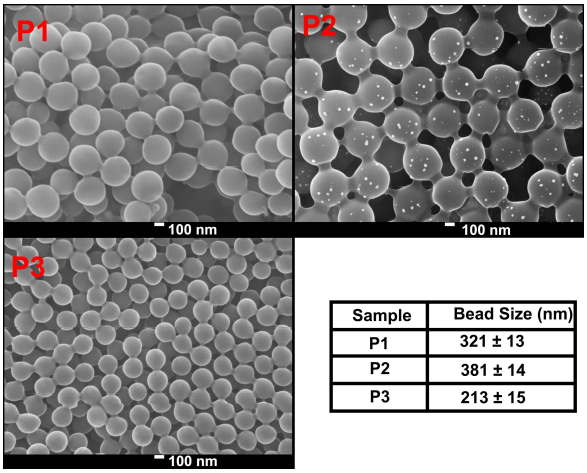

Sample	Bead Size (nm)
P1	321 ± 13
P2	381 ± 14
P3	213 ± 15

Fig. 6. SEM images of PMMA-HoVO$_4$ latexes.

SEM analysis using relatively less accelerated electrons compared to TEM was also performed to determine the composite structure. In Fig. 6, it is seen that the surface of P1 and P3 latexes is clean, while the surface of P2 latex is contaminated with salt crystals as a result of the addition of excess initiator [21]. According to this result, we can say that the nanoparticles are in the beads. However it is not possible to say anything about their distribution within the beads. In addition, when the size of the latex beads was calculated using the Image J program, it was found to be compatible with the Zetasizer NanoZS results (Table in Fig. 6).

The FT-IR spectra of pure PMMA, P1 and P3 are shown comparatively in Fig. 7. In the FT-IR analysis of all synthesized products, the characteristic spectral peaks of the PMMA were observed [25, 26]. The V–O vibration around the 760 cm^{-1}, which is the characteristic peak of HoVO$_4$ nanoparticles, is difficult to see due to the intense peaks of PMMA in this region. However, it can be said that C–H stretch bands are affected by $HoVO_4$, especially since there is an expansion in the FT-IR spectrum at the peaks from 2850 cm^{-1} to 3000 cm^{-1} compared to pure PMMA. The fact that this effect is more pronounced when the nanoparticles are added after the polymerization begins, indicates that $HoVO_4$ nanoparticles may have reacted not only with radicals but also with oligomeric species. For a better examination, the FT-IR spectra of the samples have been repeated at the magnification of the peaks between 1500 cm^{-1} and 600 cm^{-1} in Fig. 7B, where the peaks are dense and changes are observed. In the P1 latex, nanoparticles have not caused any change in the structure of PMMA. However, for P3 latex, an expansion at the peaks of 1387 cm^{-1} and 1063 cm^{-1} is observed. These peaks represent the vibrations of α-CH_3 group and the characteristic vibrations of the PMMA chain. Thus, it can be said that $HoVO_4$ nanoparticles, which were added later, made some changes in the PMMA chain.

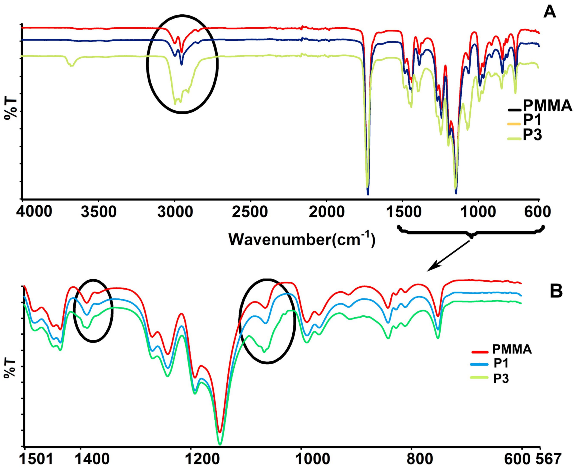

Fig. 7. FT-IR spectra of PMMA, P1 and P3. A) 4000 cm^{-1} to 600 cm^{-1}; B) 1500 to 600 cm^{-1}.

Fig. 8A shows the FT-IR spectra of the samples of PMMA, P1 and P2 in the range of 600 cm^{-1} to 4000 cm^{-1}, and Fig. 8B shows the enlarged FT-IR spectra of the samples in the range of 1500 cm^{-1} to 600 cm^{-1}. Accordingly, doubling of the initiator amount increased the intensity and width of the peaks representing the vibrations in the C–H bonds in the range of 2850 cm^{-1} to 3000 cm^{-1}. In addition, as shown in Fig. 8B, the peak at 1387 cm^{-1} representing the α-CH_3 vibrations is enlarged and slightly forked. The peak around 1100 cm^{-1}, which is one of the characteristic absorption bands of PMMA, is significantly enlarged and exacerbated. All these changes signify the presence of reactions between $HoVO_4$ and persulfate radicals.

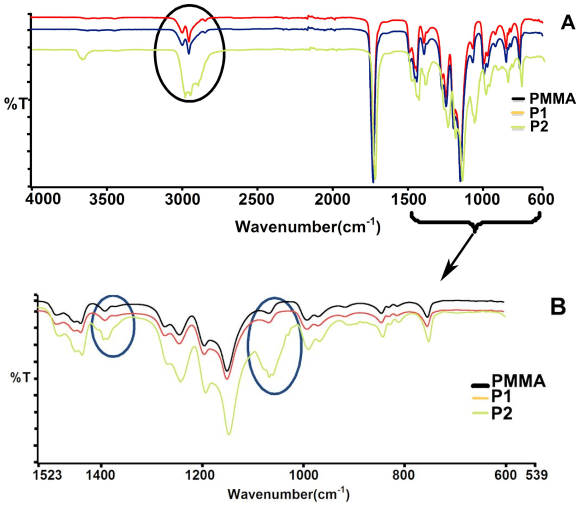

Fig. 8. FT-IR spectra of PMMA, P1 and P2. A) 4000 cm^{-1} to 600 cm^{-1} B) 1500 cm^{-1} to 600 cm^{-1}.

To eliminate the effect of vanadium-persulfate interaction, as another method, a pure PMMA latex and $HoVO_4$ dispersion were mixed at 1:1 ratio at room temperature. FT-IR spectra of the prepared composite latex are given in the range of 4000 cm^{-1} to 600 cm^{-1} in Fig. 9. The changes in the FT-IR analysis of the products obtained by the in situ polymerization method were not found in the FT-IR spectrum of the product obtained by the blending method. Besides, the characteristic peak of $HoVO_4$ which represents the vibration of the V–O bonds at 768 cm^{-1}, is clearly seen in the FT-IR spectrum (Fig. 9). Thus, it indicated that the nanoparticles were actually consumed by radicals in the medium and their concentrations decreased in the polymerization method.

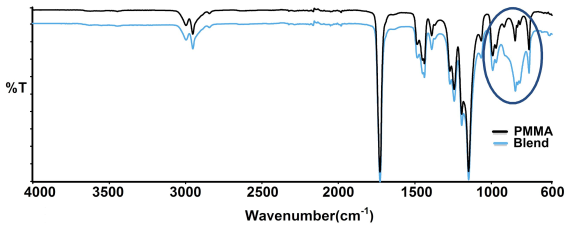

Fig. 9. FT-IR spectra of PMMA and the sample prepared by blending method.

Pure PMMA, HoVO$_4$ and all composite latexes were excited by a laser at 349 nm. Luminescence characterization was performed at the wavelengths between 340 nm and 1000 nm, using three different currents (1.8 A, 2.5 A and 3.2 A) of the laser power supply.

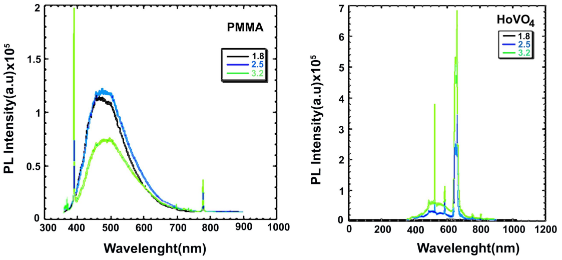

Fig. 10. Photoluminescence spectra of PMMA and HoVO$_4$ nanoparticles; insets show the currents of the laser power supply used.

As seen from the photoluminescence spectrum in Fig. 10, the PMMA shows a broad band spectrum at 520 nm due to strong light absorption in the UV region. For wide bands, generally n → π∗ or π → π∗ transitions can be formed in near UV and visible region. As shown in Fig. 10, the luminescence measurements of HoVO$_4$ nanoparticles yielded 4 characteristic luminescence peaks of Ho^{+3}; 2 in visible region and 2 in NIR region. These peaks are at 590 nm ($^5S_2$, $^5F_4 \rightarrow {}^5I_8$) and 650 nm ($^5F_5 \rightarrow {}^5I_8$) in the visible region and at 750 nm ($^5F_4 \rightarrow {}^5I_7$) and 800 nm ($^5F_2 \rightarrow {}^5I_6$) in the NIR region [27, 28].

The photoluminescence spectra of all synthesized PMMA-HoVO$_4$ nanocomposites are shown in Fig. 11. Generally, luminescence regions with similar wavelengths as PMMA may have increased PL efficiency. However, it has been determined that the peak intensity at the 650 nm, which is the characteristic Ho-peak, is different for each composite. When HoVO$_4$ nanoparticles were added to the polymerization before the start of the reaction (P1 sample), the intensity of the peak decreased. This reduction was more prominent with increasing the amount of the initiator (P2 sample). In addition, the increase in the broadband intensity of the PMMA in Fig. 11 is an interesting and important finding suggesting that some vanadium ions may be involved in the structure of PMMA. Thus, it is understood that the radical reaction affects the optical properties of the latexes.

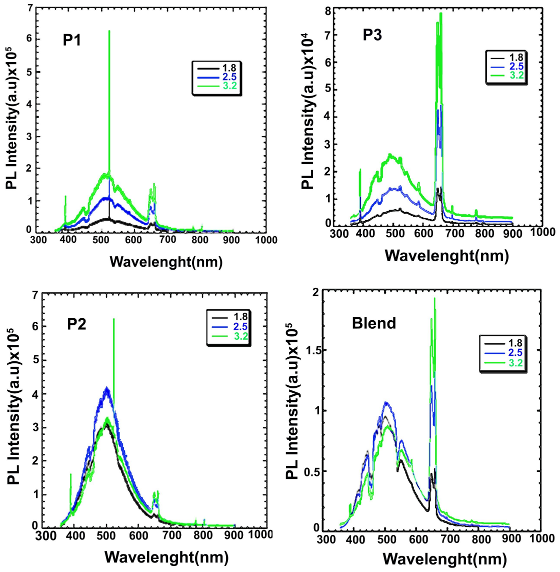

Fig. 11. Photoluminescence spectra of P1, P2, P3 and samples prepared by blending method; insets show the currents of the laser power supply used.

4. Conclusions

PMMA-HoVO$_4$ nanocomposites were synthesized by using emulsifier-free emulsion polymerization of methyl methacrylate in the presence of potassium persulfate. Vanadium ions on the surface of the nanoparticles reacted with persulfate ions and produced excessive radicals, which led to accelerated termination of the radicals. Thus the polymerization rate and yield reduced due to HoVO$_4$ nanoparticles. The size of spindle-like

$HoVO_4$ nanoparticles decreased from ∼60 nm to 30 nm and their shape turned to spherical due to radical effects in the polymerization system. The structure of the PMMA chains was also affected by the interaction of vanadium-persulfate. It was found that $HoVO_4$ nanoparticles changed the luminescence properties of the PMMA forming a new material with different properties. Thus, this study is important because it discloses a new type of initiator system for the radical polymerization. It is also a preliminary study for PMMA-vanadate nanocomposites obtained by *in situ* polymerization method.

Acknowledgements

This work was supported by the Balikesir University Research Project, Grant No. BAP 2016/154.

References

[1] Huynh W.U., Dittmer J.J., Alivisatos A.P., *Science*, 295 (5564) (2002), 2425.

[2] Yang H., Ren Q., Zhang G., Chow Y.T., Chan H.P., Chu P.L., *Opt. Laser Technol.*, 37 (4) (2005), 259.

[3] Yuwono A.H., Xue J., Wang J., Elim H.I., Ji W., Li Y., White T.J., *J. Mater. Chem.*, 13 (6) (2003), 1475.

[4] Mataki H., Yamaki S., Fukui T., *Jpn. J. Appl. Phys.*, 43 (8S) (2004), 5819.

[5] Althues H., Simon P., Kaskel S., *J. Mater. Chem.*, 17 (8) (2007), 758.

[6] Chai R., Lian H., Li C., Cheng Z., Hou Z., Huang S., Lin J., *J. Phys. Chem. C*, 113 (19) (2009), 8070.

[7] Boyer J., Johnson N., Van Veggel F., *Chem. Mater.*, 21 (10) (2009), 2010.

[8] Musbah S.S., Radojević V.J., Borna N.V., Stojanović D.B., Dramićanin M.D., Marinković A.D., Aleksić R.R., *J. Serb. Chem. Soc.*, 76 (8) (2011), 1153.

[9] Demir M.M., Koynov K., Akbey Ü., Bubeck C., Park I., Lieberwirth I., Wegner G., *Macromolecules*, 40 (4) (2007), 1089.

[10] Moynihan S., Deun Van R., Binnemans K., Krueger J., Von Papen G., Kewell A., Crean G., Redmond G., *Opt. Mater.*, 29 (12) (2007), 1798.

[11] Tan J., Zhao G., Zeng Z., Winnik M. A., *Macromolecules*, 48 (11) (2015), 3629.

[12] Bulbul B., Beyaz S., *Mater. Chem. Phys.*, 173 (2016), 200.

[13] Bünzli J.-C.G., Piguet C., *Chem. Soc. Rev.*, 34 (12) (2005), 1048.

[14] Aboumarzouk O.M., Somani B.K., Monga M., *Int. Braz. J. Urol.*, 38 (3) (2012), 298.

[15] Tücks A., Beck H. P., *Dyes Pigments*, 72 (2) (2007), 163.

[16] Yu C., Yu M., Li C., Zhang C., Yang P., Lin J., *Cryst. Growth Des.*, 9 (2) 2008, 783.

[17] Miller F.A., Wilkins C H., *Anal. Chem.*, 24 (8) (1952), 1253.

[18] Stuart B., *Infrared spectroscopy: fundamentals and applications*, Wiley-VCH, 2004.

[19] Fang G., Wu W., Deng Y., Zhou D., *Chem. Eng. J.*, 323 (2017), 84.

[20] Fang G., Wu W., Liu C., Dionysiou D.D., Deng Y., Zhou D., *Appl. Catal. B- Environ.*, 202 (2017), 1.

[21] Can S., Tanrisever T., *J. Appl. Polym. Sci.*, 103 (4) (2007), 2494.

[22] Tanrisever T., Okay O., Sönmezoğlu I.Ç., *J. Appl. Polym. Sci.*, 61 (3) (1996), 485.

[23] Zou D., Aklonis J., Salovey R., *J. Polym. Sci. Pol. Chem.*, 30 (11) (1992), 2443.

[24] Xie G., Zhang Q., Luo Z., Wu M., Li T., *J. Appl. Polym. Sci.*, 87 (11) (2003), 1733.

[25] Lin Z., *Analysis and Identification of Infrared Spectrum of the Polymer*, Sichuan University Press, Chengdu, 1989.

[26] Duan G., Zhang C., Li A., Yang X., Lu L., Wang X., *Nanoscale Res. Lett.*, 3 (3) (2008), 118.

[27] Guhur A., Jackson S.D., *Opt. Express*, 18 (19) (2010), 20164.

[28] Venkateswarlu M., Mahamuda S., Swapna K., Prasad M.V.V.K.S., Rao A.S., Shakya S., Babu A.M., Prakash G.V., *J. Lumin.*, 163 (2015), 64.

Received 2018-11-20
Accepted 2019-04-23